Intrachain dynamics and interchain structures of polymers: A comparison of polyacetylene, polyethylene, polyaniline, and poly(paraphenylene vinylene)

J. Ma,* J. E. Fischer,† E. M. Scherr,‡ and A. G. MacDiarmid‡
Laboratory for Research on the Structure of Matter, University of Pennsylvania, Philadelphia, Pennsylvania 19104-6272

M. E. Józefowicz and A. J. Epstein
Department of Physics and Department of Chemistry, Ohio State University, Columbus, Ohio 43210-1106

C. Mathis and B. Francois
Institut Claude Sadron, 67083 Strasbourg CEDEX, France

N. Coustel† and P. Bernier
Groupe de Dynamique des Phases Condensées, Université des Sciences et Techniques du Languedoc, 34060 Montpellier CEDEX, France
(Received 21 May 1991)

X-ray data for *trans*-polyacetylene $(CH)_x$ in the range 129 K< T < 513 K show that the a parameter expands twice as fast as b, accompanied by a 6° increase in the setting angle. Polyethylene $(CH_2)_x$ exhibits a similar behavior (but in the opposite sense), such that for both materials the interchain packing becomes closer to that of a two-dimensional triangular lattice at high temperature, as would be expected for close-packed disks. In contrast, poly(paraphenylene vinylene) and the emeraldine-base form of polyaniline both show small, nearly isotropic interchain thermal expansions, and the packing does not approach close packing of disks at high T. We suggest that for polymers consisting of relatively flat and rigid chains, the average interchain structure reflects the T-dependent interchain dynamics, specifically rigid-chain rotational modes about the chain axes. This effect is absent in materials for which ring torsion modes are the lowest-energy deformations. The coupling between rotational and translational degrees of freedom, and between intrachain dynamics and the average interchain structures, is discussed in light of the planar-rotor model of Choi *et al.* and the rotator phases observed in finite-length alkanes.

Polyacetylene [$(CH)_x$], polyaniline (PANI) and their doped derivatives have been extensively studied, both for their interesting electronic and magnetic properties and because they provide realizations of anisotropic guest-host systems with competing interactions. In contrast to layered materials, polymers exhibit weak bonding in two, and strong bonding in one direction, with the added feature that the chains can also rotate about their long axes, e.g., in response to doping or temperature changes. In general, the interchain degrees of freedom have not been taken into account in considering the electronic transport properties, which depend sensitively on intrachain and interchain order.[1,2] In common with many polymers, the interchain configuration of pristine *trans*-$(CH)_x$ forms a herringbone pattern, shown in the inset to Fig. 1. Upon doping, the herringbone symmetry transforms to a triangular or square arrangement, with reduced-symmetry local [chain + dopant] motifs depending on dopant size.[3] The evolution to these structures from pristine $(CH)_x$ can be realized in such a way that chain rotations and translations are successively activated. Moreover, these structural changes can be well correlated with changes in electronic and transport properties of the system.[4] A generalized anisotropic-planar-rotor (GAPR) calculation, in which the chains are modeled as rigid rotors on a two-dimensional lattice, reproduces the pristine herringbone structure with correct setting angle as well as the observed triangular symmetry obtained with small dopants.[5,6]

From a more general point of view, isotropic particles interacting with any pairwise potential in two dimensions will always be expected to pack into a triangular lattice. This is a consequence of the absence of frustration in the three-dimensional counterpart. Polyacetylene, like most linear polymers, can be viewed as quasi-two-dimensional in the plane normal to the chain axis. The projected mass density of a chain onto this plane is more nearly elliptical than disklike. The top part of the inset to Fig. 1 shows the (a,b) plane-projected rectangular structure of *trans*-$(CH)_x$,[7] while the lower part shows that the chain centers approximate a triangular lattice. With $a \approx 4.05$ Å, $b \approx 7.39$ Å at 300 K,[8] b is only 5% longer than required by $b/a = \sqrt{3}$ for a perfect triangular lattice.[9] The setting angle ϕ (the angle between the major axis of the chain projection and the longer cell axis) is about 55° at 300 K and may vary with preparation methods and degree of

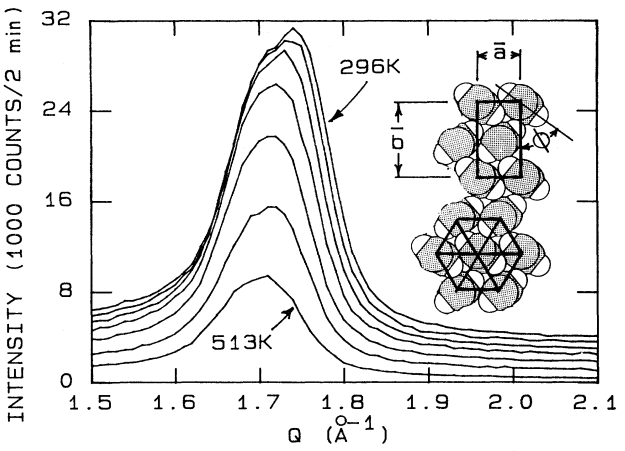

FIG. 1. X-ray diffraction of the *trans*-$(CH)_x$ (020),(110) doublet, recorded at (from top to bottom): 296, 324, 363, 408, 448, and 513 K. Inset: (a,b) plane-projected structure, after Refs. 1, 7, and 8—upper part based on the true monoclinic cell, lower part showing approximately triangular 2D lattice.

isomerization.[10]

We report here the results of x-ray experiments on *trans*-$(CH)_x$ in the temperature range 129 K$< T <$ 513 K, and on the emeraldine-base form of PANI in the range 135 K$< T <$ 296 K. From these, we derive the T dependences of a, b, and ϕ for $(CH)_x$ and of a and b for PANI. $(CH)_x$ is an example of a rigid-chain polymer; the high energy cost of π/σ hybridization ensures a high degree of chain planarity. Conversely, the chains in PANI are constructed of benzenoid and quinoid rings; easy thermal activation of ring torsions about the chain axis suggests that the projected mass density of PANI chains will be more nearly disklike than rodlike. We compare our results with similar data for two other polymers, namely polyethylene $(CH_2)_x$ and poly(paraphenylene vinylene) (PPV). The former is structurally very similar to $(CH)_x$ except for the extra hydrogen, while the phenyl and vinyl rings in PPV suggest at least a steric resemblance to PANI. We also make comparison with the literature on short-chain alkane rotator phases, in the context of coupling between intrachain dynamics and average interchain packing in quasi-2D structures.

A typical *trans*-$(CH)_x$ x-ray powder pattern consists of $\sim$ 12 Bragg peaks and some amorphous contribution.[7] Despite the limited degree of crystallinity in all forms of PANI, a reasonable structural model has been derived from powder data.[11] In both materials, the determination of interchain structural parameters is facilitated by the fact that $(HK0)$ reflections are generally much more intense than $(00L)$'s and (HKL)'s. We present in detail our data for $(CH)_x$, on which we performed two different experiments to cover the T range above and below 300 K. We used a two-axis diffractometer with 1.5-kW Cu sealed tube source, vertically-focusing graphite monochromator and single detector preceded by a Soller slit. Figure 1 shows the (020)-(110) doublet recorded at various T's above 296 K. These data were obtained from an unoriented film 100 μm thick, mounted in an evacuated radiation-heated furnace equipped with 180° access beryllium window. At 296 K the two components are barely resolved while at 513 K the apparent narrowing of the doublet indicates that the separation between them has decreased. For a triangular lattice these two reflections are exactly superimposed, so $(CH)_x$ is clearly becoming more triangular as T increases. This is also reflected by the fact that the trailing edge downshifts faster with increasing T than the leading edge (a must expand faster than b). The 296-K profile is unchanged after cooling from 513 K, apart from a very small decrease in Bragg intensity accompanied by an increase in amorphous background.

Similar data were obtained below 296 K from a partly oriented film prepared by the Akagi liquid crystal method,[12] using a miniature Joule-Thompson cold finger cryostat[13] with a beryllium vacuum shroud. The preferred orientation was characterized by a c-axis mosaic distribution of about 45° (full width at half maximum). Figure 2 shows the $(HK0)$ profile at 129 K, along with a least-squares fit. We used a powder model to fit both oriented and unoriented data in order to avoid systematic errors, having verified that the weak finite-L model intensities had negligible effects on the fitted parameters from the oriented film. The model is the monoclinic $P2_1/n$ cell[8] with freely varying a, b, and ϕ, using a Lorentzian function with equal width for all peaks. We included a much broader Lorentzian centered at ≈ 1.6 Å^{-1} to represent a variable amorphous contribution, and an isotropic Debye-Waller factor with equal amplitude for C and H. The fact that the peak position for the amorphous part is close to that for the low-index interchain crystalline peaks suggests that the interchain distance in the two forms is not drastically different. In general, the lattice constants are well defined by the peak positions, while ϕ also depends on relative amplitudes. It was found dur-

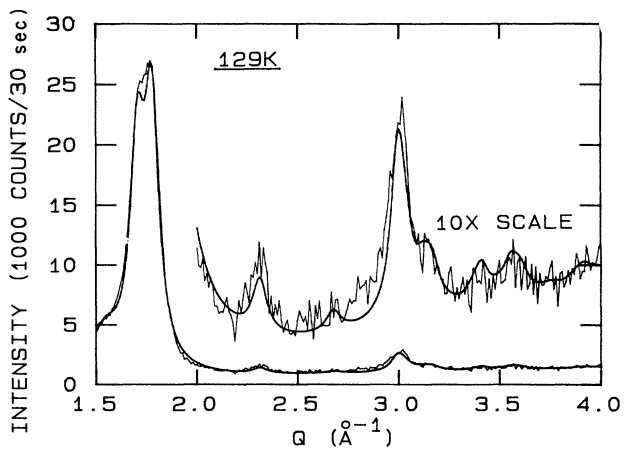

FIG. 2. Full profile of $(CH)_x$ at 129 K (light curve) and model fit (heavy curve—see text).

ing the fitting that the Debye-Waller factors varied more between two samples than with T for a given sample, indicating that static disorder dominates thermal motion in determining the Q-dependent amplitudes. However, the apparent decrease in intensity with increasing temperature (Fig. 1) may also suggest an important effect of thermal disorder, as discussed below.

Error estimates for the fitted quantities were determined after the least-squares optimization by fixing each parameter in turn at a value different from its optimal one, allowing the others to vary freely and examining the effect on the fit quality. The absolute uncertainties which result are ± 0.01 Å for a and b, $\pm 2°$ for ϕ; the relative accuracies are considerably better. The model gives a good fit over the whole T range, for both oriented and unoriented samples. We considered the possibility of paracrystalline disorder[14] in fitting the profiles, and found that a lattice constant standard deviation of 0.06 Å gives as good a fit as a model neglecting this effect. The effects of a paracrystalline fluctuation of this magnitude are comparable to the effects of a coherence length in a model of perfect but finite crystallites. Furthermore, the peak widths do not vary significantly with T as would be expected if paracrystalline disorder were important.[14]

In Fig. 3(a) we plot the T-dependent relative changes in a and b for $(CH)_x$ (open circles and squares, respectively), normalized to 129 K. The closely spaced points near 300 K indicate good overlap between fitted parameters from the two films. The initial slope of $\Delta b/b$ gives a linear expansion coefficient 4.5 x 10^{-5}/K (comparable to the c-axis value for graphite) while a expands at twice that rate. Thermal expansion is usually driven by lattice anharmonicity, the expansion coefficient vanishing as $T \rightarrow 0$ and diverging as $T \rightarrow T_m$. In the temperature range studied, we did not find any divergent behavior in either of the expansion coefficients. In fact, a slight negative curvature of both $\Delta a/a$ and $\Delta b/b$ may suggest instead a continuous approach to a high-T phase characterized by a definite b/a ratio. The top panel of Fig. 4 shows that b/a decreases from 1.83 to 1.79 as T increases from 129 K to 513 K, consistent with a tendency toward a limiting value $b/a = \sqrt{3}$. By analogy to finite chain alkanes and paraffins, we attribute this static interchain effect to the intrachain dynamics. Thermal motion in the

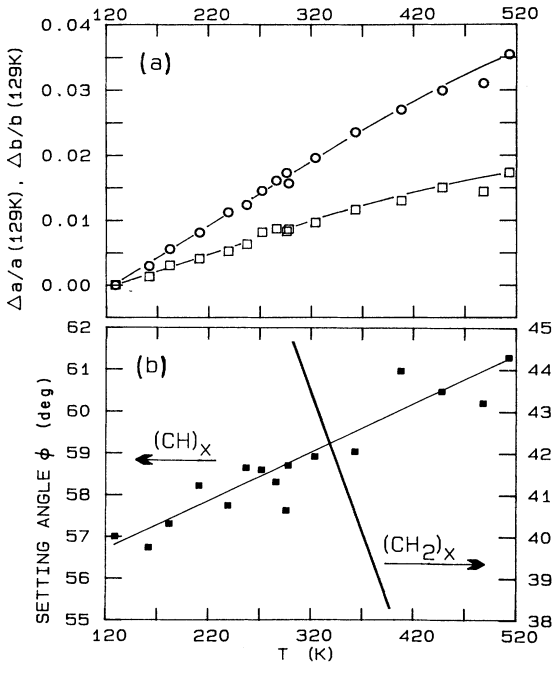

FIG. 3. T-dependent parameters of $(CH)_x$ extracted from the fits. (a) linear expansion of a and b (circles and squares, respectively), showing large anisotropy in the basal plane; (b) setting angle (filled squares). Light solid curves are guides to the eye; the heavy curve in (b) is a schematic representation of the polyethylene data from Ref. 17.

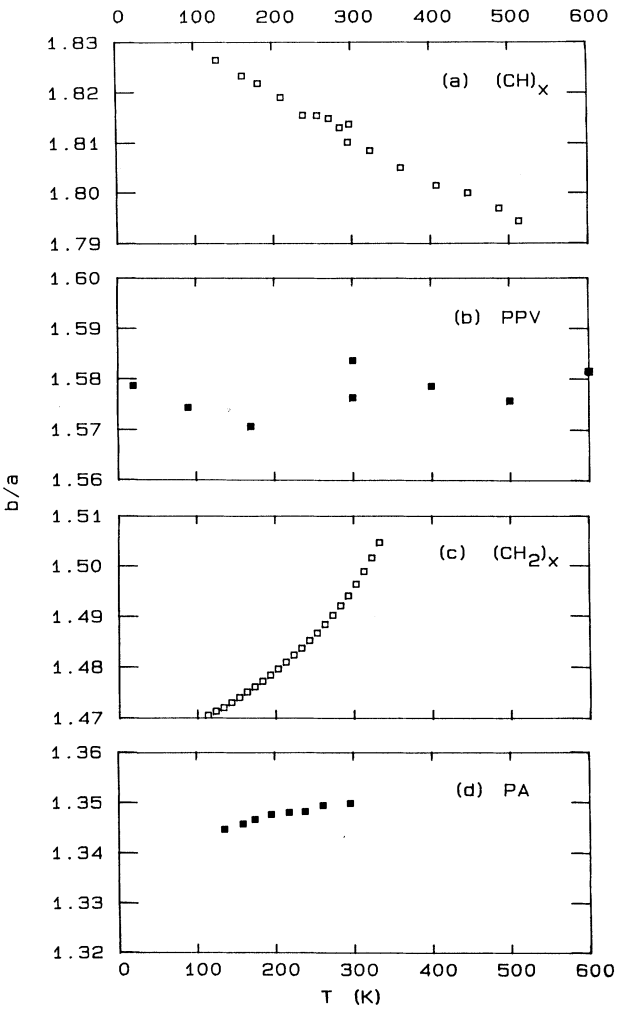

FIG. 4. T-dependent b/a ratios for four linear chain polymers. (a) $(CH)_x$ (this work), (b) PPV (unpublished data by M. J. Winokur), (c) $(CH_2)_x$ from Ref. 17, and (d) PA (this work).

(a,b) plane makes the thermally averaged chain projections more circular with increasing T, and weakens the static interchain correlations. This is the driving force by which the chain packing gradually approaches a triangular lattice.[15]

Thermally driven chain rotations can also contribute to the decrease in Bragg intensity with increasing temperature, Fig. 1. Assuming that each (rigid) chain exhibits free rotation about its axis, x-ray diffraction from the 2D lattice will reflect spatial correlations among smooth tubes of charge,[16] and thermal disorder will be due only to fluctuations in the positions of the tube centers. A more realistic assumption is that chain rotations are restricted by interchain interactions. The T-dependent intensity can still be represented by a (more complicated) Debye-Waller factor which includes *coupled* rms thermal fluctuations in ϕ and the position coordinates. Our analysis shows a Q dependence consistent with a simple Debye-Waller factor, which in principle mixes the effects of (sample-dependent) static disorder and thermal fluctuations. On the other hand, the strong T dependence of the (020)-(110) Bragg intensity cannot be explained solely by static disorder. Since this issue is not crucial to our conclusions, a detailed analysis along the lines outlined above was not attempted.

The fact that the *instantaneous* chain projections are more nearly elliptical than circular implies that the rotational and translational degrees of freedom are coupled, at least on a short time scale. The time-averaged high-T limit, a triangular lattice of disks, would be expected to expand isotropically—rotations would be irrelevant. We are clearly below this limit even at 513 K since b/a still exceeds $\sqrt{3}$ (Fig. 4), ϕ (thermally averaged) increases from 57° at 129 K to 62° at 513 K, Fig. 3(b), and a still expands faster than b, Fig. 3(a). Note from Fig. 1 (inset) that the actual projections and packing geometry *require* the expansion to be anisotropic if ϕ is allowed to vary; an increase in ϕ forces a to expand more than b, as observed, and vice versa. The net anisotropy is the sum of both effects: the consequence of (static) chain rotation and the (dynamic) thermally driven tendency toward triangular symmetry and close packing.

Polyethylene $(CH_2)_x$ has a molecular structure similar to that of $(CH)_x$, and crystallizes in the same herringbone arrangement of chain projections. But the temperature dependence of the interchain structure is drastically different.[17–19] The ratio of long to short basal cell parameters is 1.5 at 300 K (i.e., the long axis is too *short* for a triangular cell), the long axis expands *faster* than the short one, and ϕ *decreases* with increasing T, opposite to $(CH)_x$. The expansion is both larger and much more anisotropic [Fig. 4(c)], and ϕ decreases by 7° in a 100-K interval [solid curve in Fig. 3(b)]. It is, however, interesting to note that *both* $(CH)_x$ and $(CH_2)_x$ respond to increasing temperature in such a way that the interchain packing approaches a triangular lattice. For $(CH_2)_x$ the high-T approach to a more nearly circular electron density distribution has been directly observed.[20]

The differences between $(CH)_x$ and $(CH_2)_x$ can be rationalized in light of the previous discussion. In $(CH)_x$ the positional degrees of freedom are already within 4% of the asymptotic limit at 300 K, so the dominant effect of heating is chain *rotation*, which is accounted for by the GAPR model. On the other hand, $(CH_2)_x$ at low T is much farther from the asymptotic limit, so the *positional* parameters change more rapidly with increasing T (driven by intrachain dynamics), the average ϕ decreasing coincidentally. As with $(CH)_x$, the sense of $b(T)/a(T)$ defines the sense of $\phi(T)$, shown schematically by the solid lines in Fig. 4(c) and Fig. 3(b), respectively.

Finite chain alkanes $C_nH_{2n+1}R$ and paraffins C_nH_{2n+2} exhibit a progression of ordered phases with increasing T preceding melting, including for sufficiently large n a phase with perfect 2D hexagonal positional order but no orientational order, which results from the intrachain thermal averaging into disklike projections.[15] Experiments[21] and molecular dynamics simulations[22] show that the onset temperature of these "rotator phases" moves to higher T with increasing n, a consequence of increasing 3D character. In this view, an infinite chain lattice would never become truly triangular at any finite T since interchain coupling would constrain the intrachain dynamics such that the effective potentials never become pairlike, but rather always include an important angular dependence. It is interesting to note that both the idealized high-T limit of $(CH)_x$ and $(CH_2)_x$ as well as the rotator phases in finite chain alkanes, form a class of structures with positional order but no orientational order. Precisely the opposite is true in nematic liquid crystals.

A similar experiment was performed on PANI between 135 and 296 K. In this material the (a,b) lattice is far from triangular, so the (020) and (110) peaks are well separated. This permits determination of the T-dependent a and b parameters simply by fitting these two reflections with equal width Lorentzians. The results are plotted in Fig. 4(d). The b/a ratio departs more significantly from $\sqrt{3}$ than either $(CH)_x$ or $(CH_2)_x$. More importantly, there is much less anisotropy in the thermal expansion; b/a increases only slightly with increasing T and shows no evidence of an approach to high-T triangular packing. Also included as Fig. 4(b) are data for PPV, another ring-containing polymer which also shows weak or no anisotropy in thermal expansion. The vastly different behavior of PANI and PPV on the one hand, and $(CH)_x$ and $(CH_2)_x$ on the other, can be rationalized as follows. Ring-containing polymers have unique degrees of freedom, namely ring torsions,[23] which may be excited at lower T than rigid-chain twists since a smaller mass is involved. As temperature is increased, this degree of freedom gets excited before the rotation of the chain as a whole. Hence the largest thermally activated atomic motions are ring torsions, which have a less drastic effect on the projected mass density than chain twists. The comparison in Fig. 4 suggests that the difference between ring-containing polymers and rigid-planar polymers is universal, independent of whether they are conducting or insulating.[24] In principle the relative importance of the two dynamical modes can be "tuned" by varying the degree of backbone protonation or by substituting bulkier functional groups for the hydrogens.[25]

Finally we point out that the T-dependent interchain

interactions which can be inferred from our structure results imply concomitant T-dependent 3D contributions to the electronic and magnetic properties, which are most often approximated as quasi-1D.[26]

We are grateful to R. H. Baughman, P. A. Heiney, and J. P. Pouget for helpful suggestions, and especially to M. J. Winokur for graciously providing the PPV data in Fig. 4(b). This work was supported by the National Science Foundation Materials Research Laboratory Program, Grant No. DMR88-19885.

---

*Also at Physics Department, University of Pennsylvania, Philadelphia, PA 19104-6396.

†Also at Materials Science Department, University of Pennsylvania, Philadelphia, PA 19104-6272.

‡Also at Chemistry Department, University of Pennsylvania, Philadelphia, PA 19104-6323.

[1] A. J. Epstein, H. Rommelmann, M. Abkowitz, and H. Gibson, Phys. Rev. Lett. **47**, 1547 (1981).

[2] H. H. Javadi, A. Chakraborty, C. Li, N. Theophilou, D. B. Swanson, A. G. MacDiarmid, and A. J. Epstein, Phys. Rev. B **43**, 2183 (1991).

[3] P. A. Heiney, J. E. Fischer, D. Djurado, J. Ma, D. Chen, M. J. Winokur, N. Coustel, P. Bernier, and F. E. Karasz, Phys. Rev. B **44**, 2507 (1991).

[4] N. Coustel, P. Bernier, and J. E. Fischer, Phys. Rev. B **43**, 3147 (1991).

[5] H. Y. Choi, A. B. Harris, and E. J. Mele, Phys. Rev. B **40**, 3766 (1989).

[6] H. Y. Choi and E. J. Mele, Phys. Rev. B **40**, 3439 (1989).

[7] N. S. Murthy, L. W. Shacklette, and R. H. Baughman, Phys. Rev. B **41**, 12 550 (1990).

[8] C. R. Fincher, C. E. Chen, A. J. Heeger, A. G. MacDiarmid, and J. B. Hastings, Phys. Rev. Lett. **48**, 100 (1982).

[9] A different synthetic method gives films with b/a even closer to $\sqrt{3}$ at 300 K [C. Mathis, R. Weizenhofer, G. Leiser, V. Enkelmann, and G. Wegner, Makromol. Chem. **189**; 2617 (1988)]. Our results in Fig. 4 suggest quenching of a metastable high-T configuration as a possible explanation, although different ratios of *cis* to *trans* content may be important.

[10] P. Robin, J. P. Pouget, R. Comès, H. W. Gibson, and A. J. Epstein, Phys. Rev.. B **27**, 3938 (1983).

[11] J. P. Pouget, M. E. Józefowicz, A. J. Epstein, X. Tang, and A. G. MacDiarmid, Macromolecules **24**, 779 (1991).

[12] K. Akagi, S. Katayama, H. Shirakawa, K. Ataya, A. Mukoh, and T. Narahara, Synth. Met. **17**, 241 (1987).

[13] MMR Technologies, Mountain View, CA 94043.

[14] J. P. Pouget, in *Electronic Properties of Polymers and Related Compounds*, edited by H. Kuzmany, M. Mehring, and S. Roth, Springer Series in Solid State Sciences Vol. 63 (Springer-Verlag, Berlin, 1985), p. 26.

[15] D. R. Nelson and F. Spaepen, in *Solid State Physics*, edited by F. Seitz, D. Turnbull, and H. Ehrenreich (Academic, New York, 1989), Vol. 42, p. 1.

[16] P. A. Heiney, J. E. Fischer, A. R. McGhie, W. J. Romanow, A. M. Denenstein, J. P. McCauley, Jr., A. B. Smith III, and D. E. Cox, Phys. Rev. Lett. **66**, 2911 (1991).

[17] S. Kavesh and J. M. Schultz, J. Polym. Sci. **8**, 243 (1970).

[18] A. Kawaguchi, M. Ohara, and K. Kobayashi, J. Macromol. Sci. Phys. **16**, 193 (1979).

[19] G. T. Davis, R. K. Eby, and J. P. Colson, J. Appl. Phys. **41**, 4316 (1970).

[20] Masao Kakudo and Nobutami Kasai, *X-ray Diffraction by Polymers* (Kodansha and Elsevier, New York, 1972).

[21] I. Denicolo, J. Doucet, and A. F. Craievich, J. Chem. Phys. **78**, 1465 (1983).

[22] J. P. Ryckaert, M. L. Klein, and I. R. McDonald, Phys. Rev. Lett. **58**, 698 (1987).

[23] J. M. Ginder and A. J. Epstein, Phys. Rev. B **41**, 10 674 (1991).

[24] Dong Chen, M. J. Winokur, M. A. Masse, and Frank E. Karasz (unpublished).

[25] A. G. MacDiarmid and A. J. Epstein, in *Advanced Organic Solid State Materials*, edited by Long Y. Chiang, Paul Chaikin, and D. O. Cowan, MRS Symposia Proceedings No. 173 (Materials Research Society, Pittsburgh, 1990), p. 283.

[26] A. Heeger, S. Kivelson, J. R. Schrieffer, and W. P. Su, Rev. Mod. Phys. **80**, 781 (1988).